Investigation of magnetron injection locking and cascaded locking by solid-state microwave power source

Wenjie Fu, Yang Yan & Xiaoyun Li

Published online: 27 Jul 2019.

Submit your article to this journal ↗

Article views: 4

Taylor & Francis
Taylor & Francis Group

Check for updates

Investigation of magnetron injection locking and cascaded locking by solid-state microwave power source

Wenjie Fu 🆔, Yang Yan and Xiaoyun Li

School of Electronic Science and Engineering, University of Electronic Science and Technology of China, Chengdu, People's Republic of China

ABSTRACT

The investigation of injection locking of cooker magnetron by a solid-state microwave power source is reported. Experimental results show that a 2.45 GHz cooker magnetron can be locked in continuous wave operation. In the frequency-locking bandwidth, the magnetron output frequency can be tuned by adjusting the injection source. The maximum frequency-locking bandwidth of 12 MHz and noise of less than −60 dBc at a 10 kHz offset frequency are observed. Cascaded locking of multiple magnetrons is also reported. The cascaded magnetrons show the same spectrum characteristics as the solid-state microwave power source and good phase stability, which leads to high efficiency in a power combining experiment.

1. Introduction

A magnetron is a high power and high efficiency microwave vacuum tube. Benefitting from the development and popularization of microwave ovens, the 2.45 GHz cooker magnetron used in microwave ovens has become the cheapest high-power microwave source. Moreover, with the rapid growth of microwave power applications (Osepchuk 2002; Gwarek and Celuch-Marcysiak 2004), such as environmental engineering (Jones et al. 2002), drug processing (Patel and Mehta 2017), material processing (Hayn et al. 2011; Rejasse et al. 2007; Fu et al. 2019), plasma generating (Booske 2008; Uhm et al. 2006), and chemical vapor deposition (Yamada et al. 2012; Kamo et al. 1983), the cooker magnetron has become the preferred microwave source in many industrial applications, especially in economical systems.

A magnetron is a conventional vacuum microwave oscillator, and the microwave is generated when the electron beam from a cathode interacts with electromagnetic modes in a cavity resonator with a magnetic field. Unlike other vacuum tubes such as a klystron or a traveling-wave tube, the magnetron cannot function as an amplifier in order to increase the intensity of an applied microwave signal; rather, the magnetron serves solely as an oscillator. Thus, the output frequency and signal phase from the

---

CONTACT Wenjie Fu ✉ fuwenjie@uestc.edu.cn 🖳 University of Electronic Science and Technology of China, School of Electronic Science and Engineering, NO.4, Section 2, North Jianshe Road, Chengdu, Sichuan 610054, China.

magnetron is free-running (Gilmour 2011). In some applications which need to adjust or stabilize the magnetron frequency and phase, such as driving RF cavities (Chase et al. 2015; Dexter et al. 2011), chemical reactions (Fujii et al. 2014), and wireless power transfer (Shinohara et al. 2004; Takano 2013), normal magnetron control methods cannot fulfill the tasks. To realize the above functions, injection-locking has been proposed and adopted in magnetron control (Pengvanich et al. 2005; Tahir et al. 2006; Chen et al. 2018). Theoretical studies show that injection-locking needs a medium power signal to be input into the magnetron, but it has had limited applications in the past due to the lack of economical medium power microwave sources. In previous studies, self-injection (Choi and Choi 2007), peer-to-peer (Cruz et al. 2009), and master-slave (Chen et al. 2018) methods which adopt magnetrons as the source to realize two-magnetron phase-locking have been studied, but the performances and applications are limited. In recent years, with the development of laterally diffused metal oxide semiconductor (LDMOS) and GaN devices (FitzPatrick 2013), the cost and efficiency of solid-state microwave power sources (SMPS) have been sufficiently reduced and improved. Thus, adopting an SMPS as the injection source to improve magnetron locking performance is economical and possible.

In this article, we present the investigation of cooker magnetrons locked by injecting power from SMPS. The aim of this study is to explore an economical approach to build a high-power microwave system whose frequency and phase can be controlled. The injection locking model is described, and a single magnetron locking experiment is presented. To control multiple magnetrons simultaneously for high power applications, a cascaded locking approach is proposed and tested.

2. Injection-locking model

In a magnetron injection-locking system, the electric field and magnetic field components of the magnetron output microwave are denoted as $Ee^{j\omega t}$ and $He^{j\omega t}$, and the electric field and magnetic field components of the injection microwave signal are denoted as $E_1 e^{j\omega_1 t}$ and $H_1 e^{j\omega_1 t}$, where ω is the frequency of the magnetron output signal, and ω_1 is the frequency of the input signal. The microwave signal in the system is represented as

$$E_t = Ee^{j\omega t}\left(1 + \frac{E_1}{E} e^{j\Delta\omega t}\right), \tag{1}$$

$$H_t = He^{j\omega t}\left(1 + \frac{H_1}{H} e^{j\Delta\omega t}\right), \tag{2}$$

$$\Delta\omega = \omega_1 - \omega. \tag{3}$$

The input microwave power is much smaller than the output microwave power, so $E_1 \ll E$ and $H_1 \ll H$. Thus, Equations (1)–(2) become
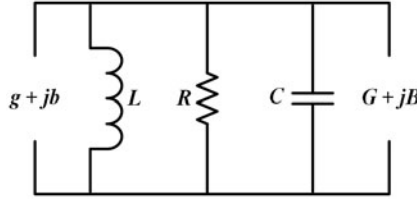
Figure 1. Equivalent circuit model of a magnetron.

$$\frac{H_t}{E_t} = \frac{H}{E}\left[1 + \left(\frac{H_1}{H} - \frac{E_1}{E}\right)e^{j\Delta\omega t}\right]. \tag{4}$$

According to the Equivalent-Circuit Method, a magnetron can be represented as an *RLC* resonant circuit (Pengvanich et al. 2005) as shown in Figure 1. In the figure, g is the electronic conductance, and b is the electronic susceptance, both of which are related to the electron beam–wave interaction inside the cavity. The admittance of the magnetron to the load is represented as $G + jB$, where G is the electronic conductance of the load, and B is the electronic susceptance of the load. The injection source can be represented as an additional slow time variety admittance $(H_1/H - E_1/E)e^{j\Delta\omega t}$. The term E_1/E represents the reflection efficiency ρ, and $H_1/H = -\rho$. The additional admittance is represented as

$$G' + jB' = \left(\frac{H_1}{H} - \frac{E_1}{E}\right)e^{j\Delta\omega t} = -2\rho e^{j\Delta\omega t}, \tag{5}$$

where G' and B' are the electronic conductance and the electronic susceptance related to the injection source. The injection source is connected to the magnetron in parallel with the load, so the total load admittance of the magnetron in the injection-locking system is

$$G_0 + jB_0 = G + jB + G' + jB'. \tag{6}$$

Set

$$\rho = |\rho|e^{j\varphi}, \tag{7}$$

$$\varphi = \Delta\omega t + \phi. \tag{8}$$

where φ is the relative phase difference between the injection signal and the output signal, $\Delta\omega$ is the frequency difference between the injection signal and the output signal which is presented in Equation (3), and ϕ is the phase difference due to the distance between input and output port. Hence, the additional admittance is of the form

$$G' = -2|\rho|\cos\varphi, B' = -2|\rho|\sin\varphi. \tag{9}$$

For free-running oscillation, the magnetron is satisfied (Yue et al. 2016; Woo et al. 1989)

$$\frac{jb}{\omega_0 C} = 2\left(\frac{\omega' - \omega_0}{\omega_0}\right) + \frac{B}{Q_L}, \tag{10}$$

where ω_0 is the cold resonant frequency of operation π mode, ω' is output frequency, and Q_L is Q value of load with magnetron cavity.

For injection-locking oscillation, the magnetron satisfies

$$\frac{jb}{\omega_0 C} = 2\left(\frac{\omega - \omega_0}{\omega_0}\right) + \frac{B}{Q_L} - \frac{2|\rho| \sin \varphi}{Q_L}, \tag{11}$$

where ω is the injection signal frequency. Substituting Equation (10) into Equation (11), we can get

$$\omega_1 - \omega' = \omega_1 - \omega + \frac{|\rho| \omega_0}{Q_L} \sin \varphi. \tag{12}$$

When the magnetron is locked, the output frequency is the same as the injection signal and $\omega_1 = \omega'$. Then, in the injection-locking condition, Equation (12) is simplified as

$$\omega - \omega_1 = \frac{|\rho| \omega_0}{Q_L} \sin \varphi. \tag{13}$$

Since $-1 \le \sin(\varphi) \le 1$, the injection-locking frequency bandwidth is satisfied as

$$|\Delta\omega| \le \frac{|\rho| \omega_0}{Q_L}. \tag{14}$$

Assuming the frequency-locked bandwidth $f_{bw} = f_{max} - f_{min}$, the Equation (14) is converter to

$$\frac{f_{bw}}{f_0} = \frac{2}{Q_L} \frac{E_1}{E} = \frac{2}{Q_L} \sqrt{\frac{P_1}{P}}, \tag{15}$$

where P_1 is the injection microwave power, P is the magnetron output power. Adler's condition (Pengvanich et al. 2005; Adler 1946) gives the required injected power P_{inject} for locking

$$P_{inject} \ge PQ_L^2 \left(\frac{f_0 - f_1}{f_0}\right)^2. \tag{16}$$

Comparing Equations (15) and (16), it shows that Equation (15) agrees with Adler's phase-locking condition.
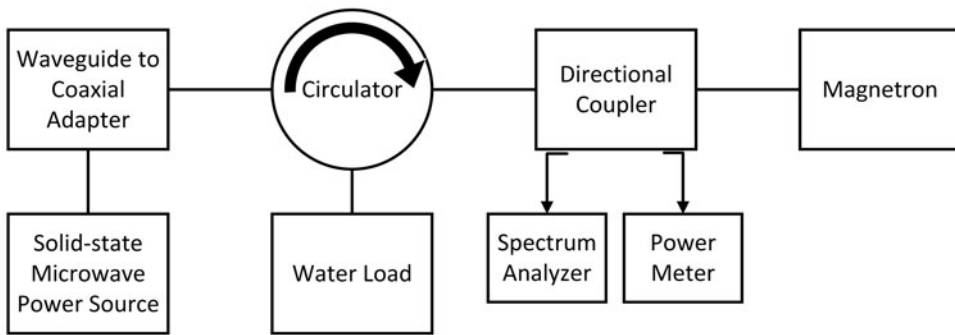
Figure 2. Single magnetron injection-locking experiment arrangement.

3. Single magnetron injection locking

To investigate cooker magnetron frequency locking characteristics, a magnetron injection-locking experiment was set up as shown in Figure 2. The magnetron used for this work was a CW Witol 2M219J magnetron, which was obtained from a domestic microwave oven. The power supply of the magnetron in the experiment was a self-made three-phase full wave rectifier with an inductance filter.

The injection microwave signal was inputted into the magnetron through a WR340 waveguide circulator, and the magnetron output power was dissipated by a matched water load. The microwave generated from the SMPS was transmitted by an N type coaxial cable and inputted into the circulator by a high-power waveguide to the coaxial adapter. The microwave that was emitted from the magnetron was transmitted to the circulator by a launcher and a waveguide directional coupler. The signals extracted from the directional coupler were used to monitor the microwave characteristics. An Agilent 8563EC spectrum analyzer was used to measure the magnetron output power and spectrum from the waveguide directional coupler. The SMPS, whose maximum power was 100 W with output power stability of better than 3%, was custom-made and manufactured by Wattsine Electronic Technology Co., Ltd (Wattsine 2019).

Figure 3 shows the measured spectrum outputs for the free-running magnetron, injection-locking magnetron, and SMPS, where the resolution and video bandwidths of the spectrum analyzer were set at 3 kHz. As shown in Figure 3a, the free-running magnetron produced an output with a broad frequency spectrum. Adjusting the operating anode voltage and anode current, the centre frequency and bandwidth of free-running oscillation varied; the centre frequency ranged from 2.442 to 2.453 MHz, and the bandwidth was about 1.5–3.0 MHz. As shown in Figure 3b, c, the injection-locking magnetron oscillated at a stable single frequency in locking status, which is same as the output frequency of the SMPS. During operation, regardless of whether the magnetron was turned on before or after the SMPS was turned on, frequency locking could be achieved. Even if the magnetron was in free-running oscillation, a stable frequency locking was observed immediately when the SMPS signal was injected.

The injection-locking characteristics of the magnetron were measured while varying the injection microwave frequency and power, and the results are shown in
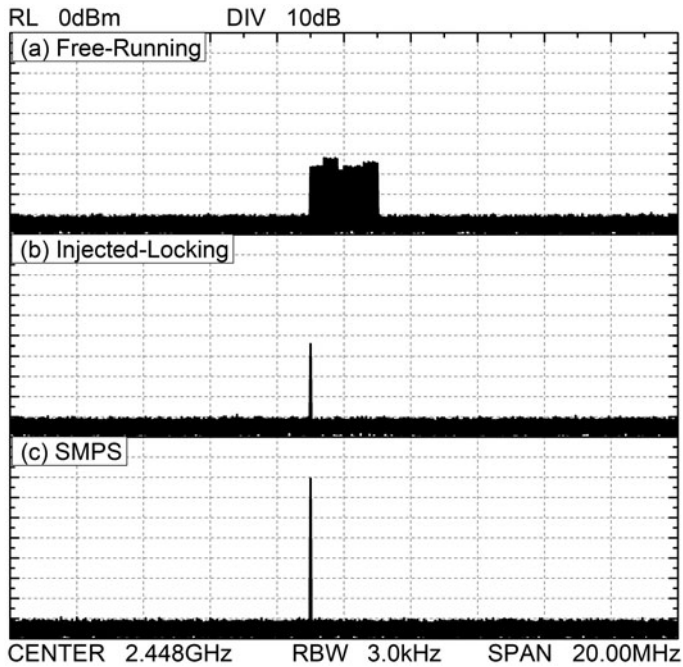
Figure 3. Frequency spectral outputs. (a) Free-running magnetron. (b) Injection-locking magnetron.
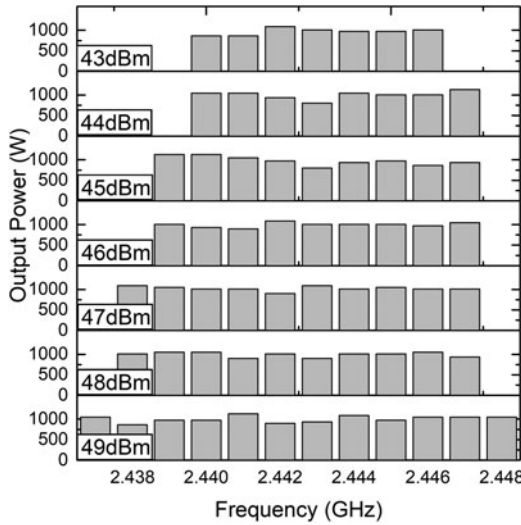

Figure 4. The experiment results of magnetron locking characteristics at different injection powers.

Figure 4, in which the magnetron anode voltage is 4200 V, and the anode current is 300 mA. To compare with the theoretical model, the injection-locking frequency region versus injection power were numerically calculated by Equation (15) and presented in Figure 5. In the calculation, f_0 was set as 2.4425 GHz, and the Q_L was ∼100, which was measured by an Agilent 8753ES S-parameter network analyzer. Both the experimental and theoretical results demonstrated that the power was higher and the
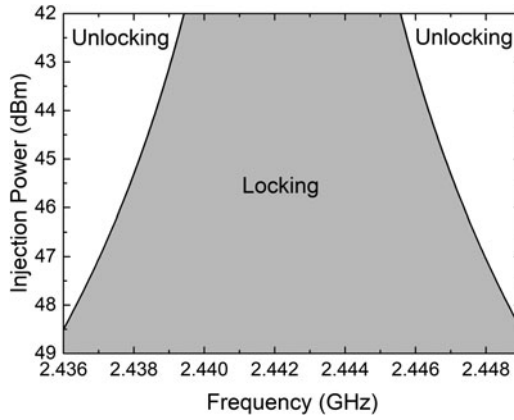
Figure 5. Numerical calculation results of the injection-locking bandwidth of magnetron.
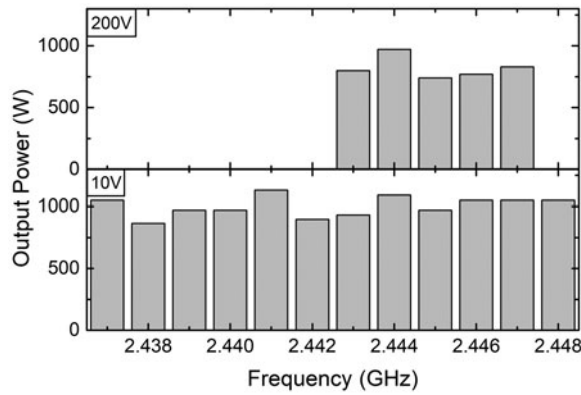

Figure 6. The experiment results of magnetron locking characteristics in different voltage ripples.

frequency-locked bandwidth was wider. The maximum frequency-locked bandwidth was measured to be 0.5%, ranging from 2.437 to 2.448 GHz. The width of the locking bandwidth showed good agreement between experiments and numerical calculations. Figure 4 indicates that the centre frequencies of the locking band were shifted at different injection powers. The experiments also show that, for the same magnetron operation voltage and current, the output power of the magnetron was different at different injection frequencies. This phenomenon indicates that the injecting power not only affected the magnetron output frequency but also affected the output power.

The free-running oscillation frequency of the magnetron is sensitive to the operating voltage. Thus, the effect of voltage ripple was investigated in this study. Two cases were tested. One case was that the power supply was a three-phase full wave rectifier without an inductance filter. The other case was that the power supply was a three-phase full wave rectifier with an inductance filter. In the first case, the voltage ripple was ∼200 V, and in the second case, the voltage ripple was ∼10 V. Both cases had an injecting power of $P_1 = 49$ dBm. The results of the two cases are shown in Figure 6, which shows that the frequency-locking bandwidth was only 5 MHz when the voltage ripple was ∼200 V, meanwhile, the frequency-locking bandwidth was 12 MHz
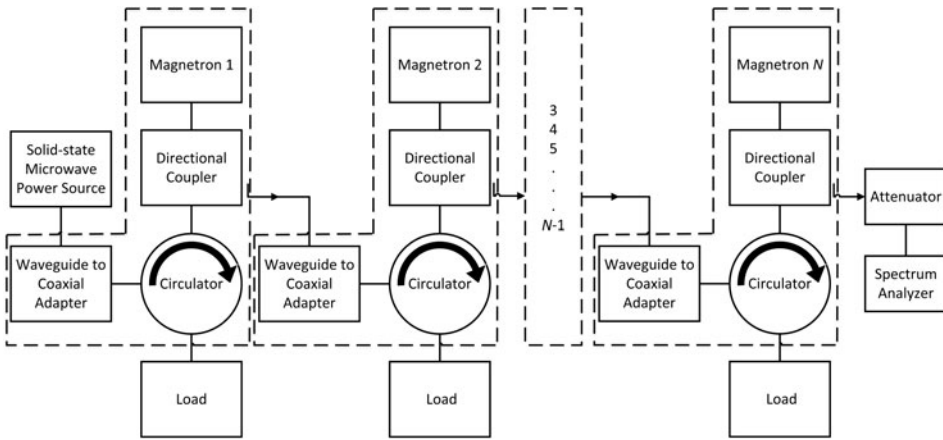
Figure 7. Scheme of cascaded magnetrons injection-locking by an SMPS.

when the voltage ripple was ∼10 V. This phenomenon indicates that the voltage ripple plays an important factor in selecting the power supply for magnetron locking. A high voltage ripple will disturb the frequency locking process, and the magnetron will not be able to be locked. Furthermore, the magnetron output power is also lower in a high voltage ripple condition than in a low voltage ripple condition. Thus, voltage ripple has to be considered in application systems design, and a half wave rectifier (Martin et al. 2001) cannot be used in injection-locking applications.

4. Multi-magnetron cascaded locking

The single magnetron locking experiment results show that the magnetron can be locked by injecting a microwave signal. For applications that need power higher than the capability of a single cooker magnetron, a multi-magnetron design could be adopted. If using one SMPS to lock multiple magnetrons, the SMPS has to generate ultra-high power, and the output should be separated to multiple channels. The ultra-high power is difficult to be achieved by current SMPS devices. To control multiple magnetrons, cascaded locking could be an economical approach. A scheme of cascaded locking is shown in Figure 7. Through a directional coupler, some of the output power from the frequency-locked magnetron can be exported and inputted into another magnetron as a locking signal. By this method, a large number of magnetrons can be locked simultaneously. The output frequencies of all magnetrons can be the same as that of the SMPS, and the frequency-locking bandwidth of the whole system is dependent on the coupled efficiencies of the directional coupler and the power of the SMPS. To achieve the highest locking efficiencies, the powers exported from the directional couplers should be the same as the SMPS output power.

To verify this approach, a power combiner experimental system with two 2M219J magnetrons was set up as shown in Figure 8 which is based on Figure 7. The outputs from the two magnetrons were connected to a WR340 waveguide power combiner, and the combined efficiency was measured to investigate the locking effect. During the experiments, the two magnetron anode voltages were 4200 V, the anode currents were 300 mA, and the output power were ∼1000 W (60 dBm). The coupling factors of
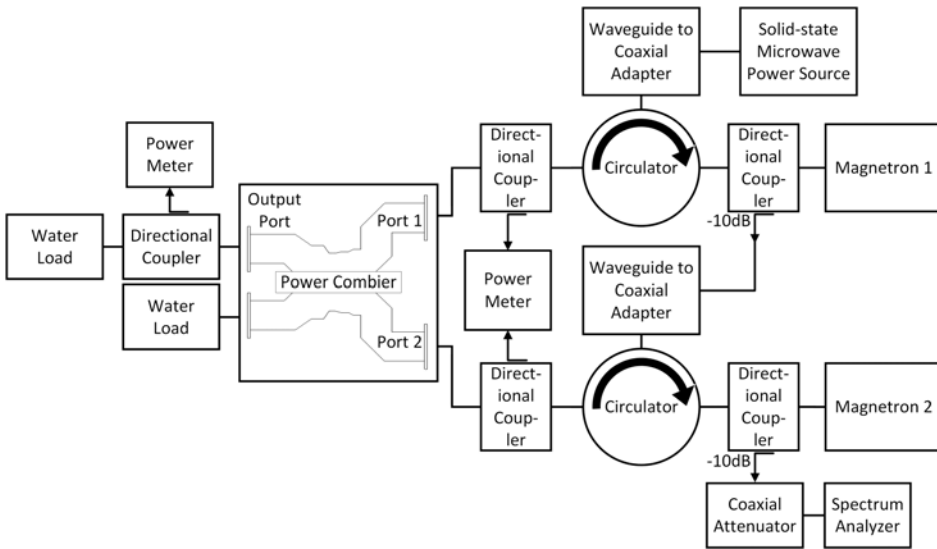
Figure 8. Scheme of power combine experimental system by two magnetrons cascaded locking.

the directional couplers for cascade connecting were −10 dB, the insertion and line losses were about −1 dB, thus the injecting power for the magnetron 2 is about 49 dBm which is similar with the injecting power for the magnetron 1 from the SMPS of 49 dBm. Two matched water load were connected to the power combiner to dissipate the combined microwave power. A 300 W coaxial attenuator was used to absorb extra power from magnetron 2, and the output powers from the two magnetrons could be equal, which is beneficial to improve the combined efficiency. Three additional directional couplers were placed in the input and output ports of the power combiner, and two Agilent E4419B power meters (Agilent Technologies, USA) with three Agilent E4413A power sensors were used to measure the power through directional couplers. The coupled factors and the insertion losses were measured by an Agilent 8753ES vector network analyzer (Agilent Technologies, USA) and considered in the combined efficiency calculation. The combined efficiency, η, was calculated by

$$\eta = \frac{P_{out}}{P_{in}^1 + P_{in}^2},\tag{17}$$

where P_{out} is the output power of the combiner, and P_{in}^1 and P_{in}^2 are the two input powers of the combiner.

The spectra of the SMPS and the second cascaded magnetron are displayed in Figure 9. The results show that the spectra of the second cascaded magnetron was the same as that of the SMPS. The noise at the 10 kHz offset frequency of the locked cascaded magnetron was smaller than −60 dBc. This demonstrates that magnetrons can be locked by cascaded connecting. Even if some cascaded magnetrons are not directly connected to the SMPS, all the magnetrons' output frequencies are the same as the SMPS output frequency, and the frequency bandwidths are also the same in the locking status.
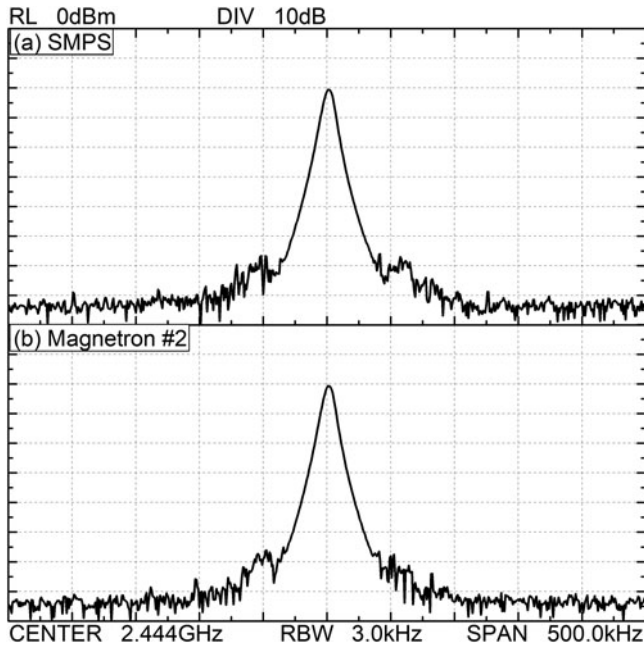
Figure 9. Frequency spectral outputs. (a) SMPS. (b) Cascaded magnetron 2.
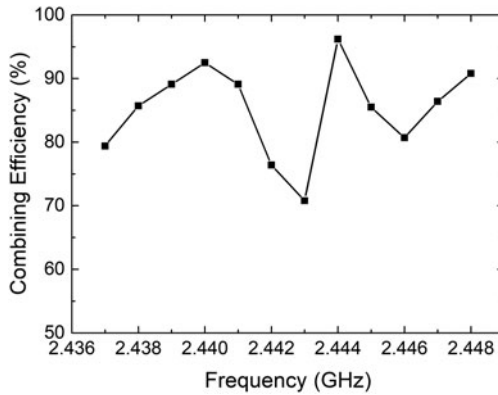

Figure 10. Combined efficiency at different frequencies.

The power combining efficiency is dependent not only upon the frequency but also upon the phase shift between magnetrons. Several coaxial cables of different lengths were prepared to connect the directional coupler and waveguide to the coaxial adapter. By changing the length of the cable and varying the SMPS frequency, the maximum combining efficiency of 96.2% was observed at 2.444 GHz in the experiment, corresponding to an output power, P_{out}, of 1864 W, in which the measured P_1 and P_2 were 980 W and 958 W, respectively. Only adjusting the output frequency of the SMPS, the experimental combining efficiency versus frequency is presented in Figure 10. During this measurement, the cable for cascade connection was not changed, so the cable length was not varied. The results indicate that the cascaded magnetrons were not only experiencing frequency locking but also phase locking.

By using a WR340 waveguide three pins tuner in the output port of power combiner, the effect of mismatching load for cascaded locking was experimented. When the output port of power combiner was mismatched, there is reflected microwave power back to input port 1 and 2. Due to circulators, the reflected microwave powers were not back to magnetrons. The reflected microwave power from port 2 was back to the directional coupler between magnetron 1 and circulator, and mostly absorbed by the directional coupler. The reflected microwave power from port 1 was back to the SMPS. When the reflected power from port 1 was not high ($<\sim$20W), the output power of the SMPS was not affected, and the magnetrons were still in locking. When the reflected power from port 1 was high, the output power of the SMPS was reduced, which resulted in the frequency-locking bandwidth was reduced and magnetrons were out of locking and back to free-running oscillation. Thus, the characteristics of the SMPS in mismatched load are a main factor of the cascaded locking.

5. Conclusion

In order to control the frequency of a cooker magnetron for economical microwave power applications, the injection-locking characteristics of a cooker magnetron were investigated. For the experiment, the injection power was generated by an affordable SMPS. The experimental results show that the magnetron can be locked by injection-locking. The frequency-locking bandwidth showed good agreement with the theoretical model. To lock multiple magnetrons simultaneously for further high-power applications, cascaded-locking was proposed and investigated. The spectra of cascaded magnetrons were consistent with that of the SMPS. A power combining experiment demonstrated that cascaded magnetrons have good performance in frequency and phase locking. This article paves the way for the development of controllable high-power microwave power application systems by using cooker magnetrons at low cost.

Acknowledgments

Funding

Notes on contributors

Wenjie Fu received the B.S., M.S. and Ph.D. degrees from the University of Electronic Science and Technology of China. He is currently an Associate Professor at the School of Electronic Science and Engineering, University of Electronic Science and Technology of China, Chengdu, China. His currently research interests include high power microwave and millimeter sources and applications.

Yang Yan received the B.S., M.S. and Ph.D. degrees from the University of Electronic Science and Technology of China. He is currently a Professor at the School of Electronic Science and

Engineering, University of Electronic Science and Technology of China, Chengdu, China. His currently research interests include high power vacuum electronics devices.

Xiaoyun Li graduated from the Tsinghua University, China, in 1979. Currently, he is a Senior Research Engineer at the School of Electronic Science and Engineering, University of Electronic Science and Technology of China, Chengdu, China. His major research interests are microwave power applications and systems, especially in microwave oven.

ORCID

Wenjie Fu   http://orcid.org/0000-0003-4321-4757

References

Adler R. 1946. A study of locking phenomena in oscillators. Proc IRE. 34: 351–357.

Booske JH. 2008. Plasma physics and related challenges of millimeter-wave-to-terahertz and high power microwave generation. Phys Plasmas. 15:055502.

Chase B, Pasquinelli R, Cullerton E, Varghese P. 2015. Precision vector control of a superconducting RF cavity driven by an injection locked magnetron. J Instrum. 10:03007.

Chen C, Huang K, Yang Y. 2018. Microwave transmitting system based on four-way master–slave injection-locked magnetrons and horn arrays with suppressed sidelobes. IEEE Trans Microwave Theory Techn. 66:2416–2424.

Choi JJ, Choi GW. 2007. Experimental observation of frequency locking and noise reduction in a self-injection-locked magnetron. IEEE Trans Electron Devices. 54:3430–3432.

Cruz EJ, Hoff BW, Pengvanich P, Lau YY, Gilgenbach RM, Luginsland JW. 2009. Experiments on peer-to-peer locking of magnetrons. Appl Phys Lett. 95:191503.

Dexter AC, Burt G, Carter RG, Tahir I, Wang H, Davis K, Rimmer R. 2011. First demonstration and performance of an injection locked continuous wave magnetron to phase control a superconducting cavity. Phys Rev ST Accel Beams. 14:032001.

FitzPatrick D. 2013. Recent development in high power solid state power amplifiers - A European Perspective. In: 2013 ARMMS RF and Microwave Society conference; Wyboston, UK, Nov. p. 1–6.

Fu W, Deng J, Li X. 2019. Microwave drying of fabrics. J Microwave Power Electromagn Energy. 53:12–23.

Fujii S, Kujirai H, Mochizuki D, Maitani MM, Suzuki E, Wada Y, Mayama N. 2014. Chemical reaction under highly precise microwave irradiation, J Microw Power Electromagn Energy. 48:89–103.

Gilmour AS. 2011. Klystrons, traveling wave tubes, magnetrons, crossed- field amplifiers, and gyrotrons. Boston (MA): Artech House.

Gwarek WK, Celuch-Marcysiak M. 2004. A review of microwave power applications in industry and research. In: 15th International Conference on Microwaves, Radar and Wireless Communications (IEEE Cat. No.04EX824); Warsaw, Poland, Vol.3. p. 843–848.

Hayn RA, Owens JR, Boyer SA, McDonald RS, Lee HJ. 2011. Preparation of highly hydrophobic and oleophobic textile surfaces using microwave-promoted silane coupling. J Mater Sci. 46:2503–2509.

Jones DA, Lelyveld TP, Mavrofidis SD, Kingman SW, Miles NJ. 2002. Microwave heating applications in environmental engineering—a review. Resour Conserv Recycl. 34:75–90.

Kamo M, Sato Y, Matsumoto S, Setaka N. 1983. Diamond synthesis from gas phase in microwave plasma. J Crystal Growth. 62: 642–644.

Martin D, Jianu A, Ighigeanu D. 2001. A method for the 2.45-GHz magnetron output power control. IEEE Trans Microwave Theory Techn. 49: 542–545.

Osepchuk JM. 2002. Microwave power applications. IEEE Trans Microwave Theory Techn. 50: 975–985.

Patel P, Mehta P. 2017. Microwave-assisted heating: innovative use in hydrolytic forced deg-radation of selected drugs. J Microwave Power Electromagn Energy. 51:205–220.

Pengvanich P, Neculaes VB, Lau YY, Gilgenbach RM, Jones MC, White WM, Kowalczyk RD. 2005. Modeling and experimental studies of magnetron injection locking. J Appl Phys. 98: 114903.

Rejasse B, Lamare S, Legoy M-D, Besson T. 2007. Influence of microwave irradiation on enzymatic properties: applications in enzyme chemistry. J Enzyme Inhib Med Chem. 22: 519–527.

Shinohara N, Matsumoto H, Hashimoto K. 2004. Phase-controlled magnetron development for SPORTS: space power radio transmission system. URSI Radio Sci Bull. 2004:29–35.

Tahir I, Dexter A, Carter E. 2006. Frequency and phase modulation performance of an injec-tion-locked CW magnetron. IEEE Trans Electron Devices. 53:1721–1729.

Takano T. 2013. Wireless power transfer from space to earth. IEICE Trans Electron. E96-C: 1218–1226.

Uhm HS, Hong YC, Shin DH. 2006. A microwave plasma torch and its applications. Plasma Sources Sci Technol. 15:26–34.

Wattsine. 2019. Solid state medium-power generator. Chengdu (China): Wattsine Electronic Technology Co., Ltd; [accessed 2019 May 10]. http://www.wattsine.com/rf-power-amplifier/Solid_state_microwave_source/34.html

Woo W, Benford J, Fittinghoff D, Harteneck B, Price D, Smith R, Sze H. 1989. Phase locking of high-power microwave oscillators. J Appl Phys. 65:861–866.

Yamada T, Ishihara M, Kim J, Hasegawa M, Iijima S. 2012. A roll-to-roll microwave plasma chemical vapor deposition process for the production of 294 mm width graphene films at low temperature. Carbon. 50:2615–2619.

Yue S, Gao D, Zhang Z, Wang W. 2016. Theoretical investigation of frequency characteristics of free oscillation and injection-locked magnetrons. Chin Phys B. 25:118403.